



HyspIRI Level-2 TIR Products and Validation: Surface Radiance, Land Surface Temperature, Land Surface Emissivity



Glynn Hulley, Simon Hook

Jet Propulsion Laboratory, California Institute of Technology, Pasadena, CA

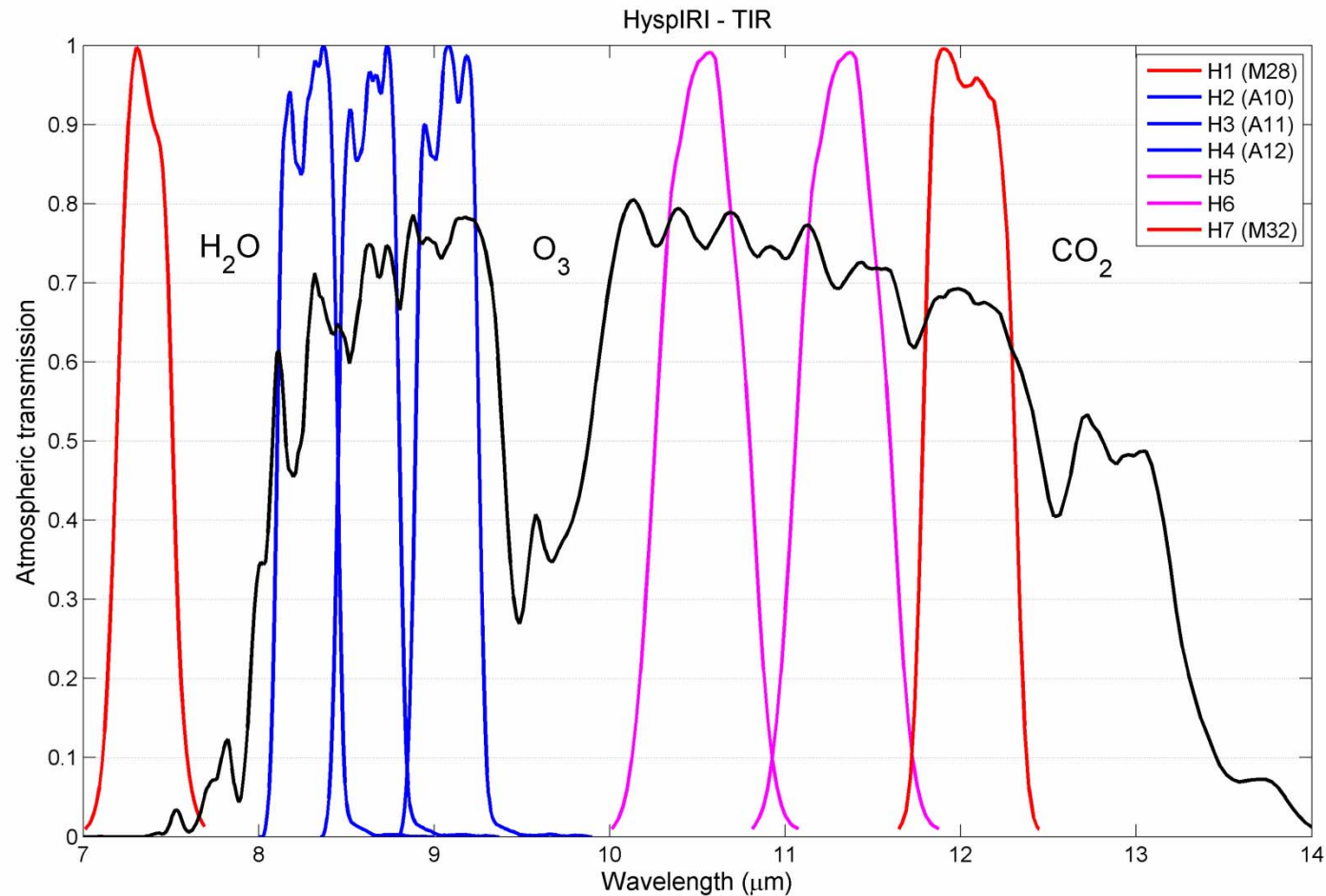
HyspIRI Workshop, Pasadena, CA, 11 August, 2009

HyspIRI - ASTER - MODIS

TIR Product Characteristics

| | HyspIRI | Terra ASTER | Terra MODIS |
|-----------------------------|------------------------|-------------------------|------------------------------------|
| Sensor Calibration: | 0.1-0.2 K | < 0.3 K | < 0.2 K |
| Cloud Contamination: | Cloud Detection | Cloud Detection | Cloud Detection |
| Retrieval Type: | TES + WVS | TES | Day/Night (V4) Split-Window(V5) |
| Temporal Sampling: | 11:00 AM, PM 5 days | 10:30 AM, PM 16 days | 10:30 AM, PM Twice daily |
| Spatial Resolution: | 60 m | 90 m | 1 km |
| Swath Width | 600 km | 60 km | 2300 km |
| View angle: | $\pm 25^\circ$ | $\pm 8.55^\circ$ | $\pm 55^\circ$ |
| MTIR Bands: | 8 bands | 5 bands | 7 bands |

HyspIRI Response Functions



Note: ASTER Spectral Library has been convolved to these response functions and will be available soon on HyspIRI website

HyspIRI TIR Level-2 Products

1. Cloud Mask

- a. Approach
- b. ASTER examples

2. Surface Radiance

- a. Infrared Radiative Transfer
- b. Atmospheric Correction
- c. Validation

3. Land/Ocean Surface Temperature and Surface Emissivity (LST&E)

- a. Algorithm Development
- b. TES examples
- c. Validation

1. Cloud Mask

- Accurate, reliable and automatic cloud detection is critical
- Use same approach as the New ASTER Cloud Mask Algorithm (NACMA)
- Hybrid algorithm, clear-sky conservative:
 - Landsat-7 two pass approach
 - MODIS shadow test
 - AVHRR thin cirrus test
- HypsIRI VSWIR repeat is 19 days, but TIR is 5 days
- Propose using VIIRS for visible data (250 m) when VSWIR not available

** Hulley G.C., S.J. Hook, 2008, A New Methodology for Cloud Detection and Classification with Advanced Spaceborne Thermal Emission and Reflection (ASTER) Data , *Geophys. Res. Lett.*, 35, L16812, doi:10.1029/2008GL034644

ASTER Cloud Spectral Tests

Table 1. Pass-1 Filters and Threshold Tests Using Reflectance, r_i and Temperature, T_{sat} , Values From Equations (1) and (2)

| Filter | Threshold Test | Function |
|-------------------------|---|--|
| 1 Brightness Threshold | $r_2 > 0.08$ | Eliminates low reflectance, dark pixels |
| 2 Snow Threshold | $NDSI = (r_1 - r_4)/(r_1 + r_4) < 0.7$ | Eliminates snow |
| 3 Temperature Threshold | $T_{sat} < 300$ | Eliminates warm surface features |
| 4 Band 4/5 Composite | $(1 - r_4)T_{sat} < 240 \Rightarrow$ snow present $(1 - r_4)T_{sat} < 250 \Rightarrow$ snow absent | Eliminates cold surfaces - snow, tundra |
| 5 Growing vegetation | $\frac{r_3}{r_2} < 2$ | Eliminates reflective growing vegetation |
| 6 Senescing vegetation | $\frac{r_3}{r_1} < 2.3$ | Eliminates reflective senescing vegetation |
| 7 Rocks and Sand | $\frac{r_3}{r_4} > 0.83$ | Eliminates reflective rocks and sand |
| 8 Warm/Cold Cloud | $(1 - r_4)T_{sat} > 235 \Rightarrow$ warm cloud $(1 - r_4)T_{sat} < 235 \Rightarrow$ cold cloud | Warm and cold cloud classification |
| Cloud Shadow | $r_3 < 0.05$ and $\frac{r_3}{r_1} > 1.1$ | Detects cloud shadows |

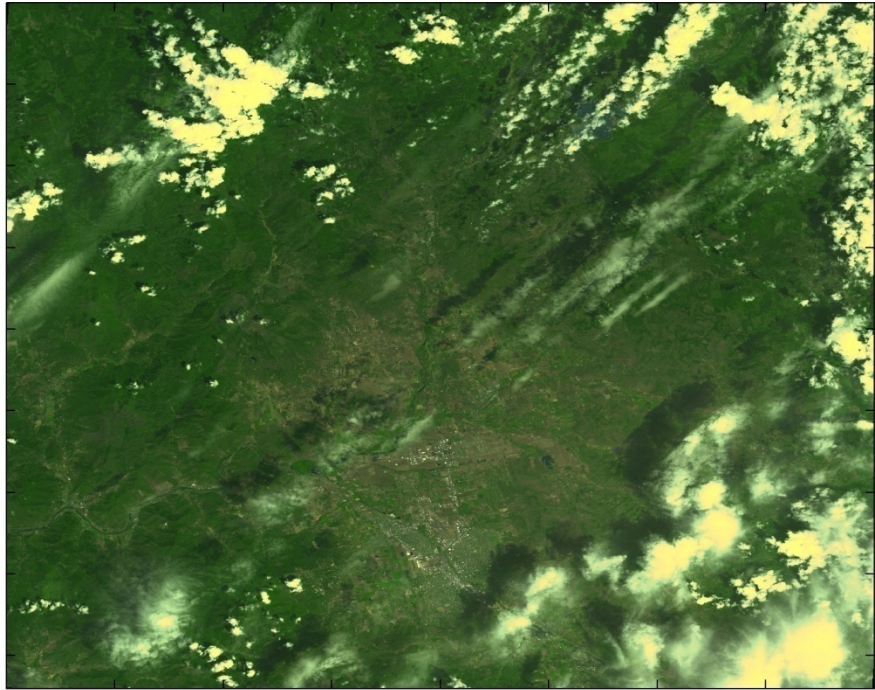
Table 2. Brightness Temperature Thresholds for the Thin Cloud/Cirrus Test

| BT _{10.6} (K) | BT _{10.6–11.3} (K) | |
|------------------------|-----------------------------|------------|
| | Snow > 50% | Snow < 50% |
| 260 | 0.55 | 0.50 |
| 270 | 1.00 | 0.51 |
| 280 | 1.20 | 0.53 |
| 290 | 1.30 | 1.00 |
| 300 | 1.50 | 2.00 |
| 310 | 3.00 | 3.00 |
| 320 | 4.00 | 4.00 |
| 330 | 5.00 | 5.00 |

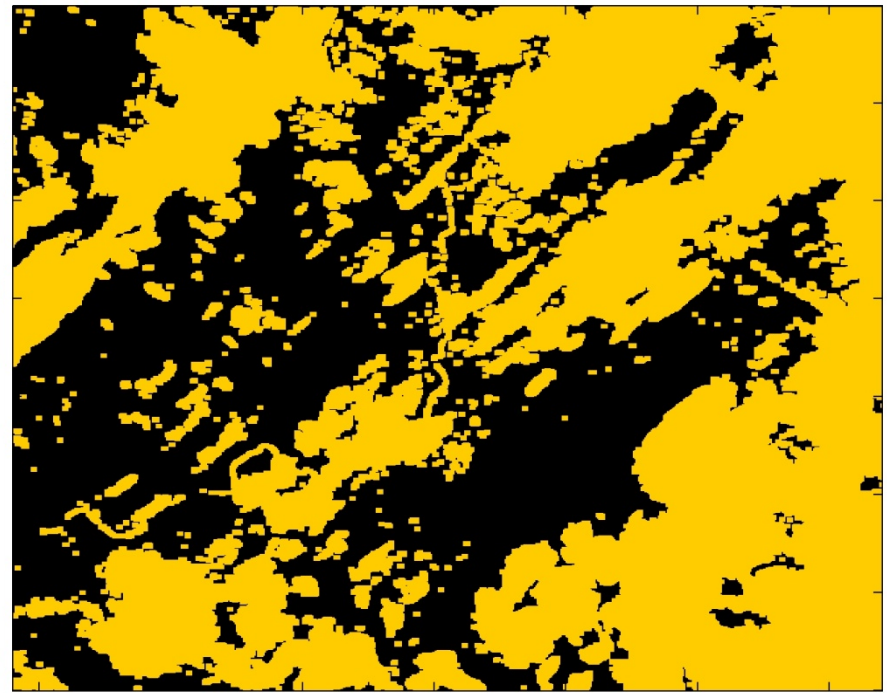
Thin cloud/cirrus test

Cumulus + thin cirrus example

ASTER visible image



ASTER Cloud Mask + Fill



Shadow – **Cyan**

Cloud – **Gold**

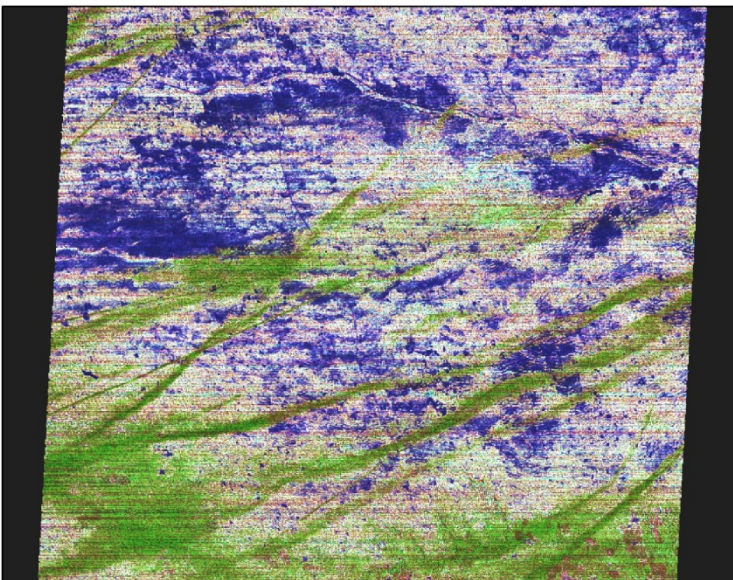
Clear – **Black**

ASTER Visible image

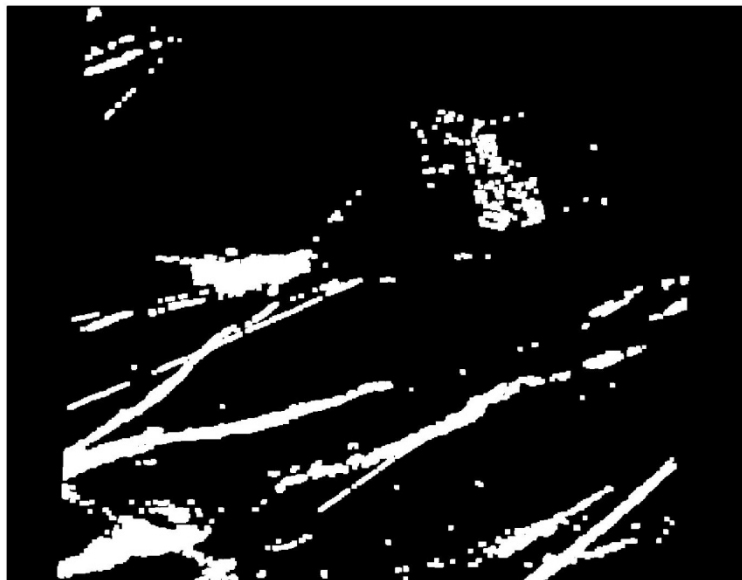


Jet Contrails
Sub-visible cirrus

Emissivity (R=10, G=12, B=14)



Cloud Mask



2. Surface Radiance

- Surface radiation is combination of direct surface emission and reflected radiance from sky and surrounding
- Atmospheric corrections necessary to isolate surface features, which are obscured by atmospheric attenuation
- Approach
 1. Choose a radiative transfer model to estimate magnitude of atmospheric emission, absorption and scattering
 - eg. MODTRAN 4, 5.3 (beta), CRTM – JCSDA
 2. Acquisition of atmospheric profiles (eg. Temperature, water vapor, ozone, aerosol) at time and location of observation
 - VIIRS (MODIS follow-on) or CrIS (AIRS follow-on) on NPP/NPOESS
 - NCEP GDAS as backup (currently used for ASTER)
 - OMI (ozone)

Infrared Radiative Transfer

$$L_i(\theta) = \underbrace{\tau_i(\theta) \cdot e_i \cdot B_i(T_S)}_{\text{Surface Emission}} + \underbrace{\tau_i(\theta) \cdot (1 - e_i) \cdot \bar{L}_i}_{\text{Surface Reflection}} + \underbrace{\int B_i(T(P)) d\tau_i}_{L_i^{atm\uparrow}}$$

Surface Radiance

Surface Emission Surface Reflection $L_i^{atm\uparrow}$

Skin Temperature & Surface Emissivity

Atmospheric Correction

Surface Radiance:

$$L_{surf,i} = e_i \cdot B_i(T_s) + (1 - e_i) \cdot$$

$$\overline{L}_i^{\downarrow} = \frac{L_i(\theta) - L_i^{\uparrow}(\theta)}{\tau_i(\theta)}$$

➤ **Atmospheric Parameters:** $\tau_i(\theta)$, $L_i^{\uparrow}(\theta)$, $L_i^{\downarrow}(\theta)$

Estimated using radiative transfer code such as MODTRAN with Atmospheric profiles and elevation data

➤ Derivation of e_i and T_s is an undetermined problem

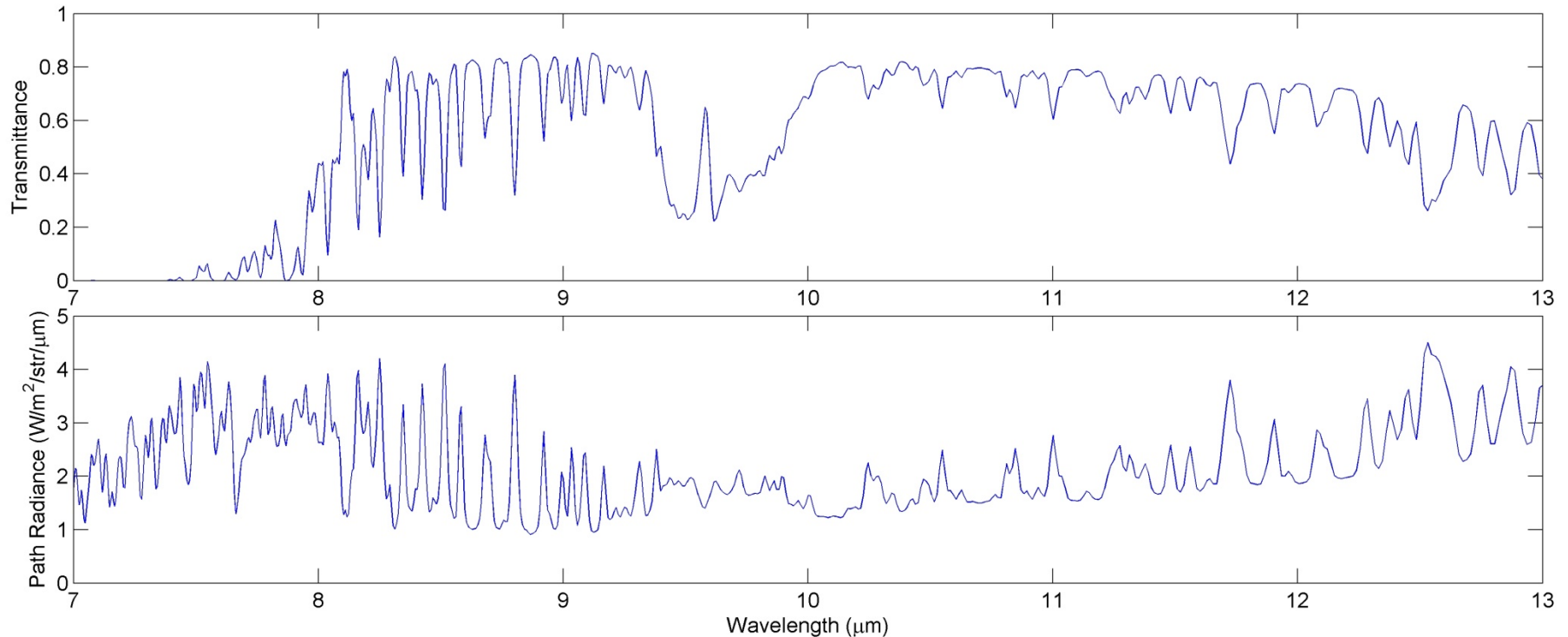
The number of parameters (T_s, e_i in N channels) is always greater than the number of simultaneous equations needed to solve the problem (N)

=>Additional, independent constraint is needed

Radiative Transfer Model

- MODTRAN 5.3 (beta)
 - Finer spectroscopy: resolution down to 0.1 cm^{-1}
 - DISORT multiple scattering speed and accuracy improved
 - Option for including auxiliary molecules
 - Several tape5 input files can be processed with single execution
- Maintain close communication with developers on updates and improvements (Gail Anderson)
- Other radiative transfer models will be explored, eg. Community Radiative Transfer MODEL (CRTM) – open source through JCSDA

Radiative Transfer Model



** Sky Radiance will be regressed from path radiance results to limit number of MODTRAN runs and minimize computational time

$$\text{eg. } L_i^\downarrow = a_i + b_i \cdot L_i^\uparrow(\theta) + c_i \cdot L_i^\uparrow(\theta)^2$$

Water-Vapor Scaling Method

Tonooka, H., (2005), Accurate Atmospheric Correction of ASTER Thermal Infrared Imagery Using the WVS Method, *IEEE Trans. Geos. Remote Sens.*, 43 (12)

EMC/WVD equation

$$\left\{ \begin{array}{l} T_{g,i} = \alpha_{i,o} + \sum_{k=1}^n \alpha_{i,k} T_k \\ \alpha_{i,k} = p_{i,k} + q_{i,k} W + r_{i,k} W^2 \quad (k = 0, 1, \dots, n) \end{array} \right.$$

Global simulation database
(NCEP and radiosondes)

$$\gamma^{a_i} = \frac{\ln \left[\frac{\tau_i(\gamma_2)^{\gamma_1^{a_i}}}{\tau_i(\gamma_1)^{\gamma_2^{a_i}}} \cdot \left(\frac{B_i(T_{g,i}) - L_i^\uparrow(\gamma_1)/(1 - \tau_i(\gamma_1))}{L_i - L_i^\uparrow(\gamma_1)/(1 - \tau_i(\gamma_1))} \right)^{\gamma_1^{a_i} - \gamma_2^{a_i}} \right]}{\ln \left(\frac{\tau_i(\gamma_2)}{\tau_i(\gamma_1)} \right)}$$

γ usually ranges from [0.8 1.6] and reduces error in water vapor profiles over graybodies (water, vegetation) used for atmospheric correction

Water-Vapor Scaling Method

Tonooka, H., (2005), Accurate Atmospheric Correction of ASTER Thermal Infrared Imagery Using the WVS Method, *IEEE Trans. Geos. Remote Sens.*, 43 (12)

γ is then horizontally interpolated and smoothed over scene, and atmospheric correction terms are updated:

Transmittance: $\tau_i(\gamma) = \tau_i(\gamma_1)^{(\gamma^{ai} - \gamma_2^{ai}) / (\gamma_1^{ai} - \gamma_2^{ai})} \cdot \tau_i(\gamma_2)^{(\gamma_1^{ai} - \gamma^{ai}) / (\gamma_1^{ai} - \gamma_2^{ai})}$

Path Radiance: $L_i^{\uparrow}(\gamma) = L_i^{\uparrow}(\gamma_1) \cdot \frac{1 - \tau_i(\gamma)}{1 - \tau_i(\gamma_1)}$

Sky Radiance: $L_i^{\downarrow}(\gamma) = a_i + b_i \cdot L_i^{\uparrow}(\gamma) + c_i \cdot L_i^{\uparrow}(\gamma)^2$

WVS example Over Tokyo Bay with ASTER data

Tonooka, (2005)

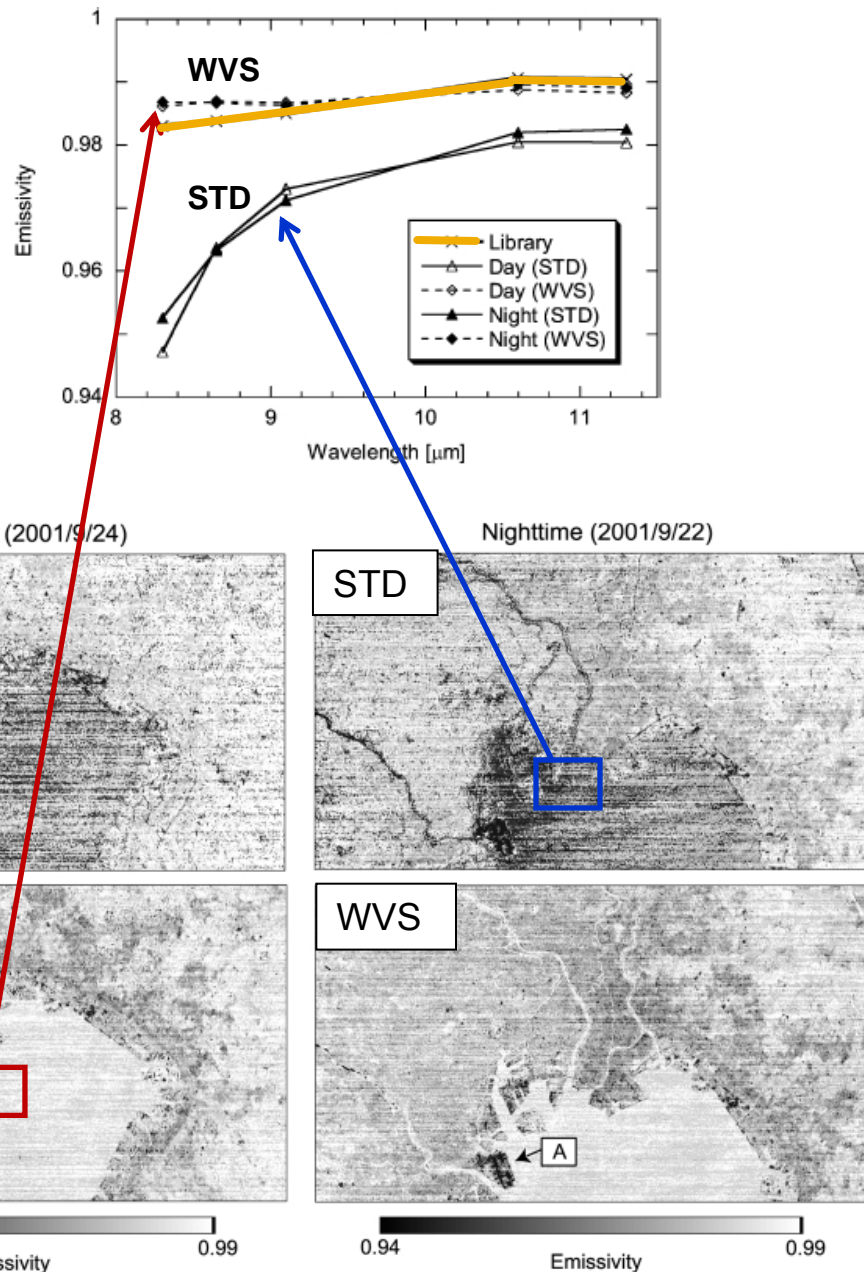
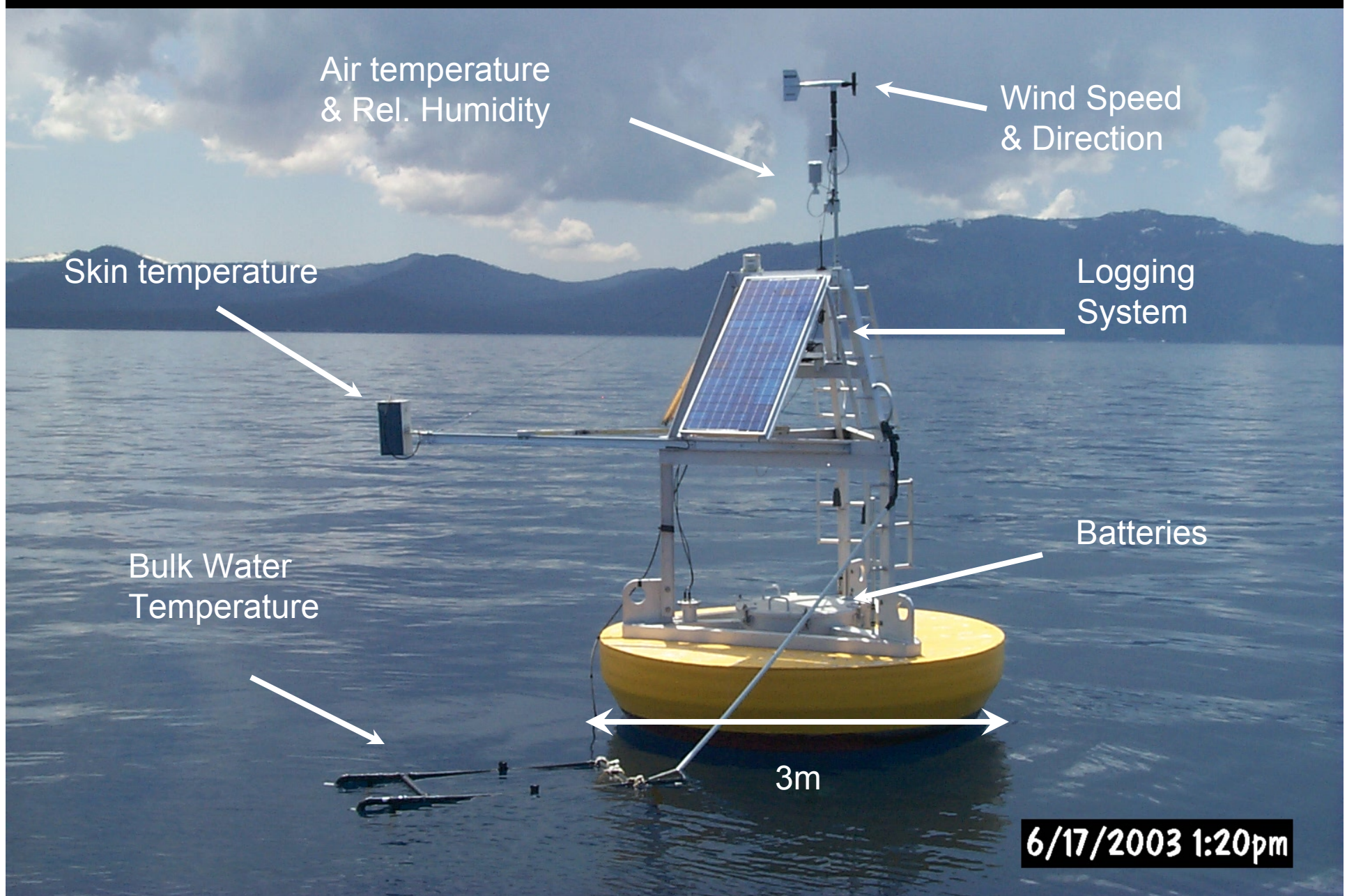


Fig. 20. Emissivity maps of band 12 retrieved from the daytime and nighttime scenes by each method.

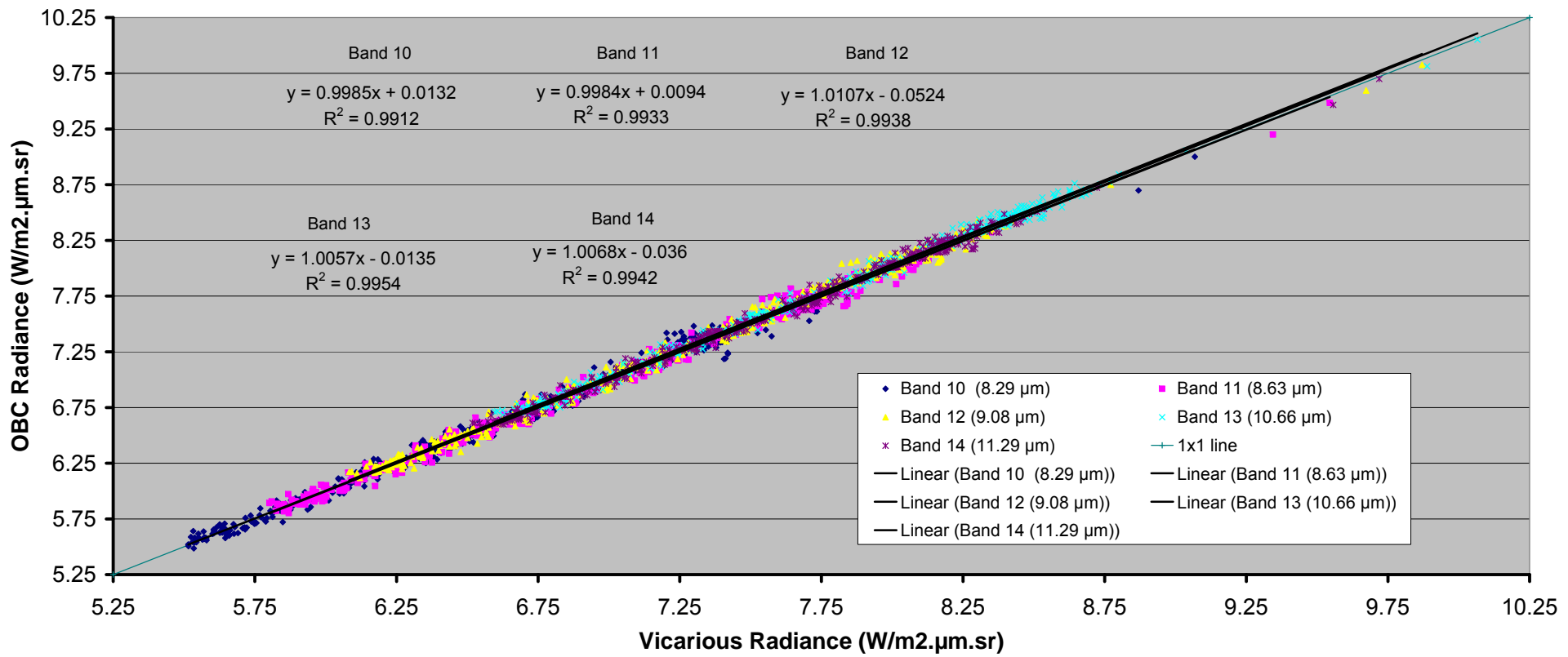
Surface Radiance: Validation

- Water Surface Targets:
 1. Lake Tahoe automatic Cal/Val facility (Cool, 0 - 25° C)
 2. Salton Sea (Hot, >30° C!)
- Land Surface Targets:
 1. DOME-Argus, Antarctica (high, and cold, <-60° C)
 2. Valencia site (>30 km²), homogenous rice fields (cool)
 3. Sand dune sites in southwestern USA (hot)
 - Emissivity measured and well characterized
 - Multiple balloon launches to control temperature and water vapor
 - Sun photometer for aerosol optical depth and column water
- Airborne Instruments
 - HyTES, MASTER

TB3 Installed 11-04-2002



ASTER Vicarious and OBC Thermal Infrared Derived Radiances at Lake Tahoe and Salton Sea CY2000-2008, v3.0x



Excellent best fit lines obtained in all bands R² is typically 0.99
 Data clearly follow 1x1 line

3. Land Surface Temperature and Emissivity (LST&E)

- Key Earth System Data Records (ESDR) in climate change studies
 - Climate modeling, estimating heat radiation budgets
 - Surface-atmosphere interactions
 - Cryospheric studies and hydrology
 - Earth surface composition and change
- Emissivity is critical for determining LST ($1.5\% = 1 \text{ K}$ error)
- Goals:
 1. Estimate accurate and precise LST ($<1 \text{ K}$)
 2. Recover accurate emissivity for mineral exploration and geologic mapping ($<1\%$)
 3. Produce seamless products, with no artificial discontinuities, which exist in split-window, land class approach.

LST&E Retrieval Algorithms

■ Split-Window/Land Class (MODIS, MOD11_L2)

Atmospheric effects reduced by combining radiances measured in two clear channels (eg. 11 and 12 μm) as in SST retrievals

➤ PROS:

- Easy and fast application once coefficients are determined
- Accurate and stable over graybody surfaces (eg. dense vegetation)

➤ CONS:

- Uncertainty in emissivity results in significant error ($0.5\% = 0.7 \text{ K}$ error)
- Emissivity is not retrieved, but assigned using Land Class
- Does not account for changes in soil moisture
- Unstable over arid and semi-arid areas, due to unknown emissivity

LST&E Retrieval Algorithms

■ Day/Night Algorithm (MODIS, MOD11B1)

Additional constraint from assuming emissivity remains constant during day and nighttime observation, while LST changes.

➤ PROS:

- LST and emissivity physically determined
- Emissivity retrieved in seven bands

➤ CONS:

- Pair of clear day/night scenes necessary
- Misregistration between day/night scenes
- Cloud effects (night scenes)
- Real emissivity differences between day/night scenes

LST&E Retrieval Algorithms

■ Temperature Emissivity Separation (TES, ASTER)

Relies on empirical relationship between spectral contrast and minimum emissivity, determined independently from laboratory measurements

➤ PROS:

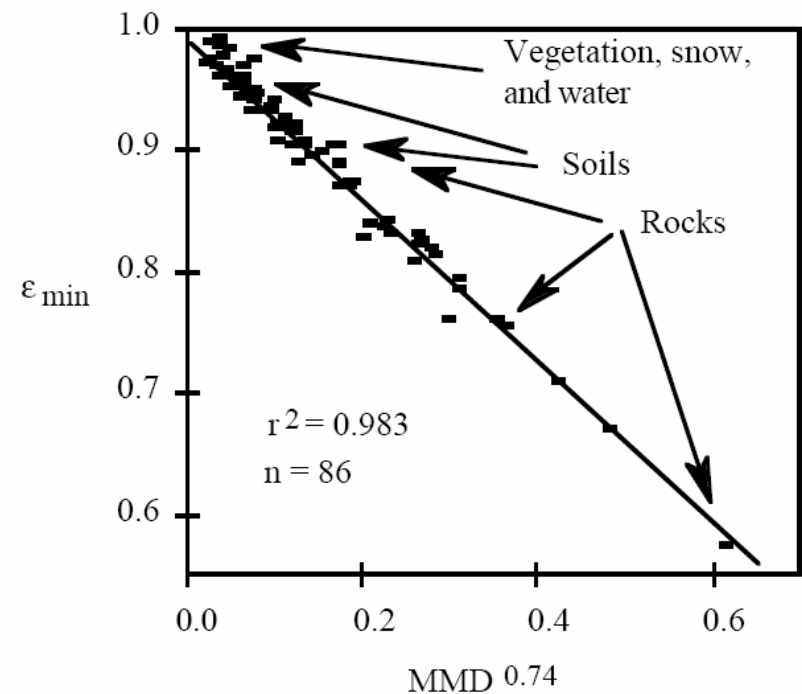
- LST and emissivity in all bands are physically determined
- High accuracy over low emissivity, high contrast areas (eg. Deserts)
- Validated with ground truth using sand dune sites to 1.6%

➤ CONS:

- Atmospheric profiles are required for atmospheric correction
- Accuracy is dependent on atmospheric correction
- Accuracy degraded over graybody surfaces as a result, since errors in atmospheric correction resulted in larger 'apparent' contrast

Temperature Emissivity Separation (TES)

- Inversion of T and ϵ are underdetermined
- Additional constraint arises from minimum emissivity vs spectral contrast
- Three error sources:
 - Reliance on empirical function
 - Atmospheric corrections
 - Radiometric calibration errors
- Reported accuracy for ASTER:
 - LST is 1.5 K
 - ϵ is 0.015 (1.5 %)

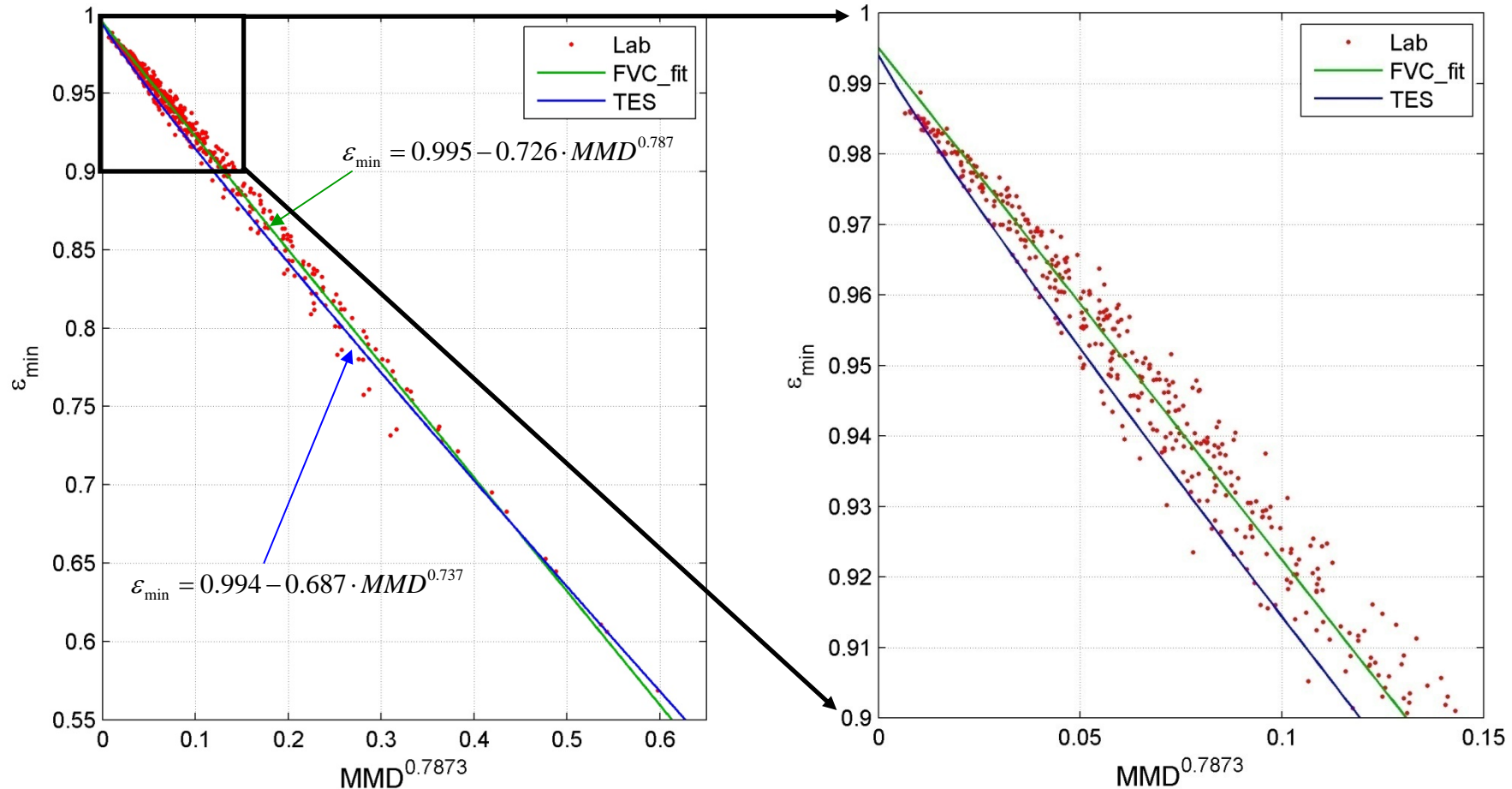


$$\epsilon_{\min} = 0.994 - 0.687 \cdot MMD^{0.74}$$

TES Vegetation Adjustment

$$\varepsilon_b = \varepsilon_b^{veg} \cdot FVC + \varepsilon_b^{soil} \cdot (1 - FVC)$$

ε_b^{veg} - Conifer spectra
 ε_b^{soil} - 59 soil/sand spectra
 FVC = 0:5:100%



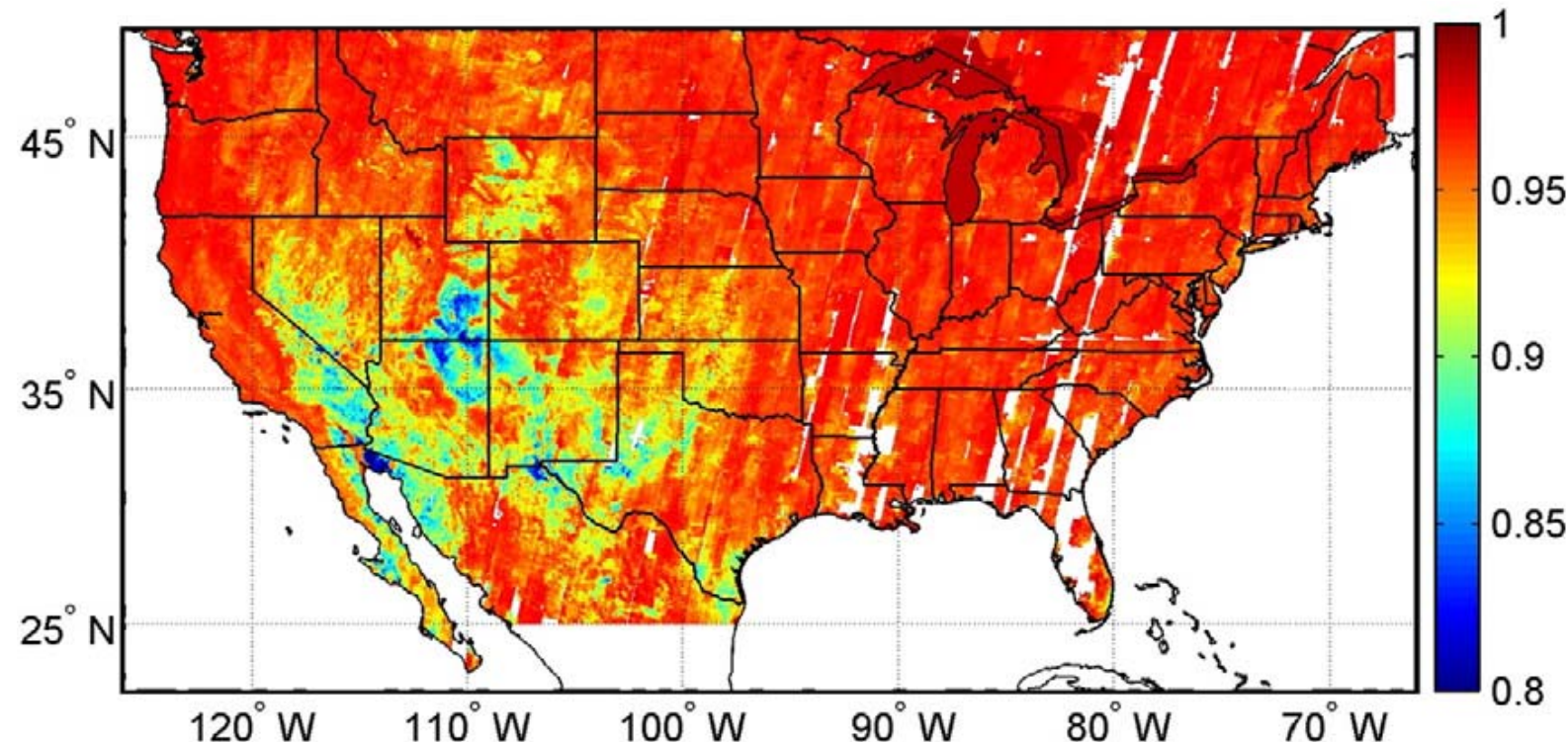
TES underestimates vegetation from 1.5-2% in emissivity

FVC curve reduces this down to <1% (~ 0.7 K)

NAALSED Mean Summer (Jul-Sep) Emissivity:

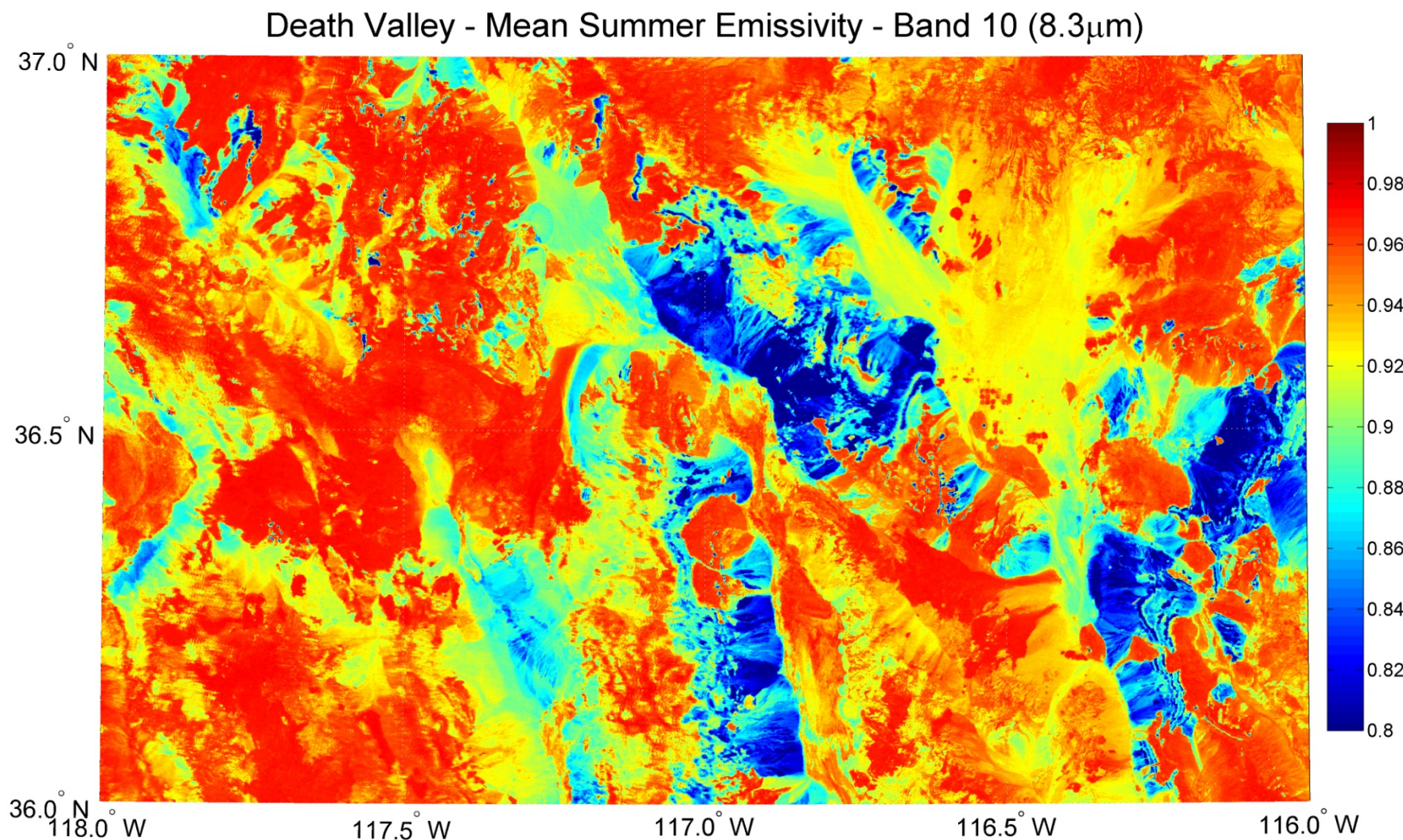
Band 12 (8.6 μ m): 2000-2008: 50,075 scenes

<http://emissivity.jpl.nasa.gov>

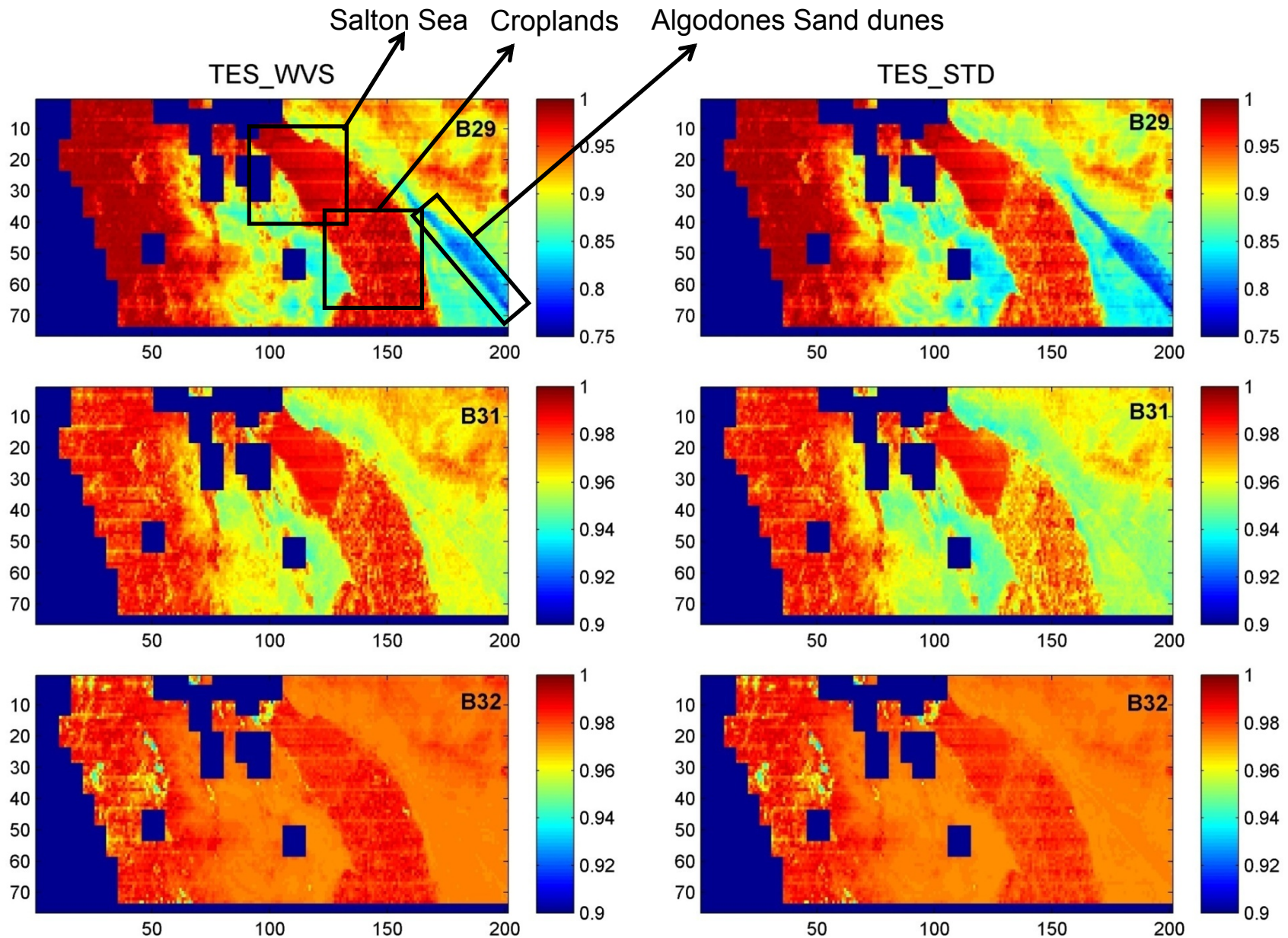


** Gaps plan to be filled during Jul-Sep 2009 ASTER acquisition

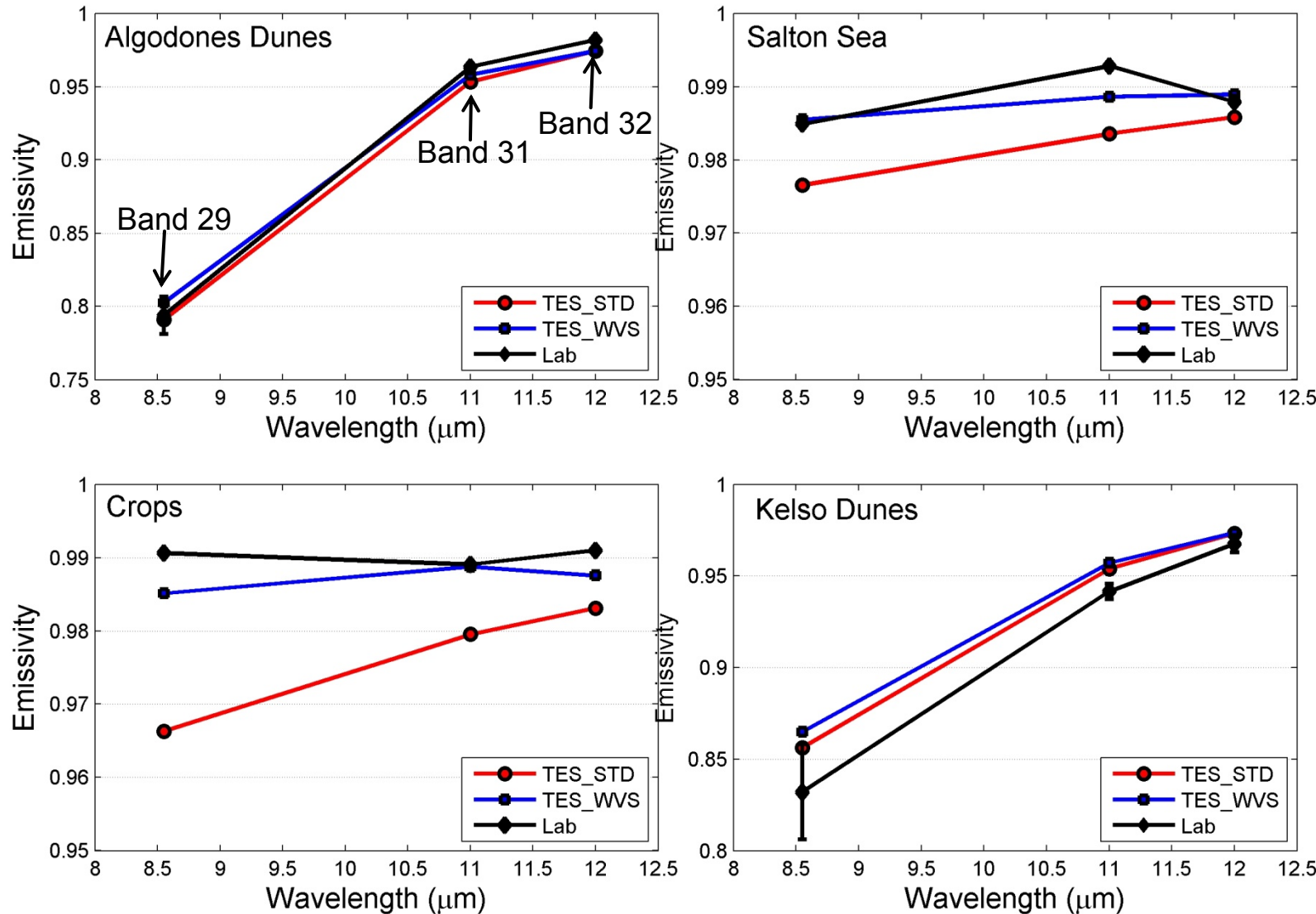
Hulley, G. C., & Hook, S. J., (2009), The North American ASTER Land Surface Emissivity Database (NAALSED) Version 2.0, *Remote Sensing of Environment*, doi:[10.1016/j.rse.2009.05.005](https://doi.org/10.1016/j.rse.2009.05.005)



TES applied to MODIS data (MOD021KM)



TES applied to MODIS data (MOD021KM)



Emissivity Validation

- HyTES – Hyperspectral Thermal Emission Spectrometer
 - 256 TIR bands
 - Simulation and algorithm development for HyspIRI
 - Expected 2011 debut
- NAALSED intercomparisons
 - ASTER emissivity database of North America
 - 100 m resolution
- Ground Truth Measurements
 - 9 pseudo-invariant sand dune sites covering broad range of emissivity in TIR (0.6 – 0.96)
 - Emissivity of samples measured in the laboratory using Nicolet spectrometer and integrating sphere (high accuracy – 0.02%)

Sand samples collected in field



Reflectance measured using Nicolet 520 FTIR spectrometer

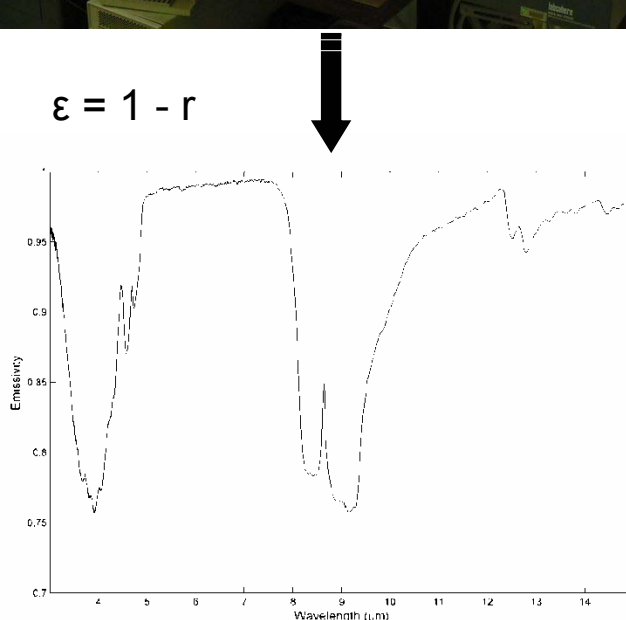


JPL
LAB MEASUREMENTS

spectral range: 2.5 – 15 μm

spectral resolution: 4 cm^{-1}

1000 scans in 10 minutes



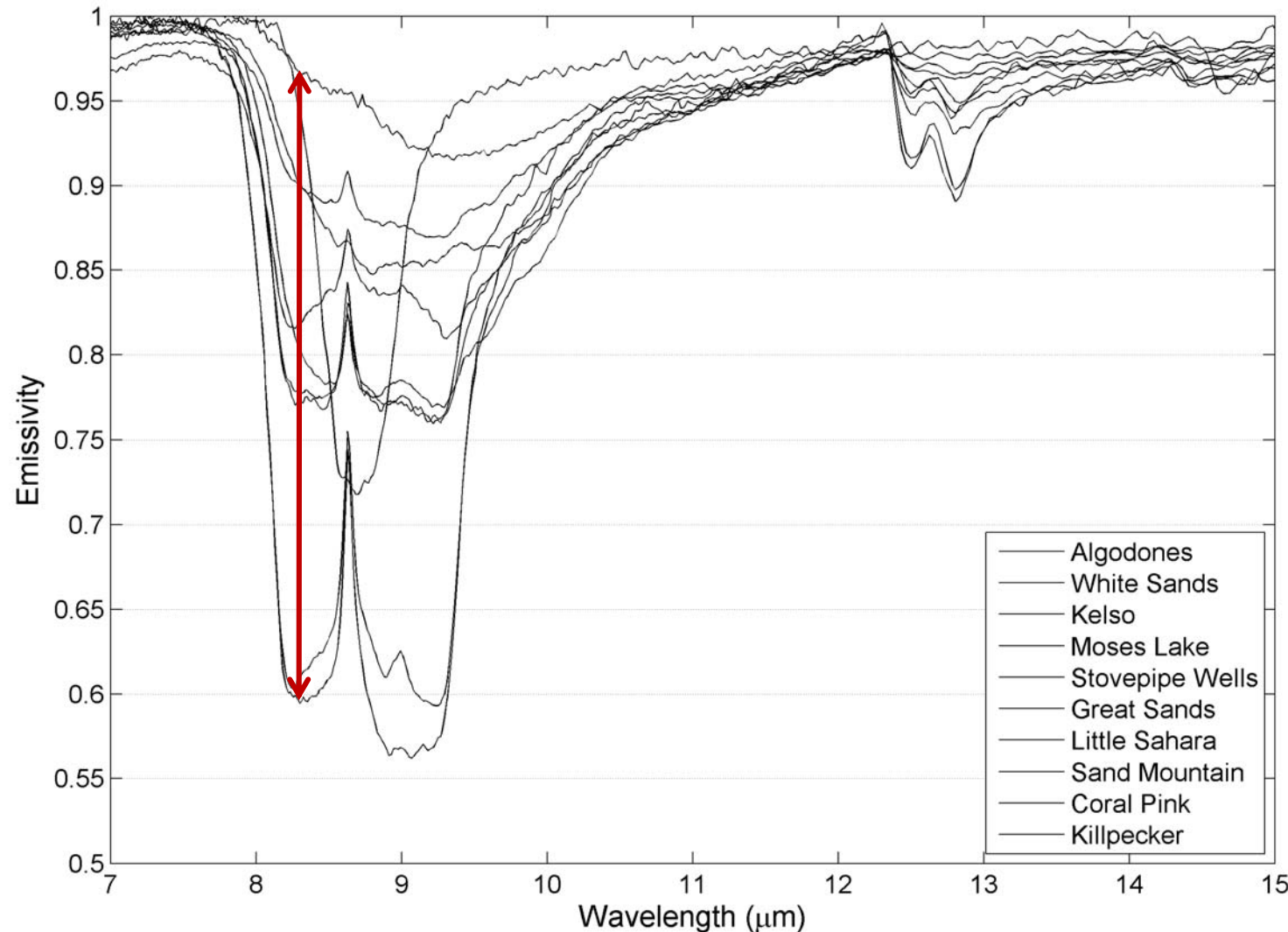
Pseudo-Invariant Sand Dune Sites

Table 1

Summary of the major characteristics of each dune site including locality, elevation, surface area, dune height, grain size, sand source and bulk mineralogy.

| Dune site | Locality | Surface area (km ²) | Elevation/max dune height (m) | Grain size | Sand source | Mineralogy (XRD) |
|---|--|------------------------------------|----------------------------------|-----------------------|--|---|
| Algodones (32.95° N, 115.07° W) | Southeast CA, Eastern margin of the Salton Trough | 720 | 94/80 | Medium to coarse sand | Beach sand from Lake Cahuilla | Major: quartz |
| Coral Pink (37.04° N, 112.72° W) | Sand Valley, just north of UT-AZ border, west Kanab | 13.6 | 1780/10 | Medium sand | Navajo, Page and Estrada Jurassic sandstones of the Vermillion Cliffs | Major: quartz |
| Great Sands (37.77° N, 105.54° W) | San Luis Valley, CO, adjacent to Sangre de Cristo, NE of Alamosa | 104 | 2560/230 | Medium to coarse sand | Quartz and volcanic fragments derived from Santa Fe and Alamosa formations, recent fluvial (Rio Grande) deposits | Major: quartz Minor: potassium feldspar |
| Kelso (34.91° N 115.73° W) | Mojave Desert, CA, southeast of Baker | 115 | 800/195 | Medium sand | Derived from sedimentary, metamorphic, igneous terrains from Mojave River alluvial apron | Major: quartz Minor: potassium feldspar |
| Killpecker (41.98° N 109.10° W) | Southwest WY, from Eden across Rock Springs into Red Desert | 550 | 2000/45 | Medium sand | Sandstone and siltstone of the Laney member of the Green River Formation | Trace: magnetite Major: quartz Trace: magnetite Minor: plagioclase feldspar, epidote |
| Little Sahara/Lynndyl (39.7° N 112.39° W) | West-central UT, Sevier River drainage basin, west of Lynndyl | 575 | 1560/200 | Fine sand | Deltaic and shoreline sediments from the Provo shoreline of Lake Bonneville | Major: quartz Minor: plagioclase feldspar, pyroxene, carbonate, magnetite |
| Stovepipe Wells (36.62° N, 117.11° W) | Central Death Valley, CA, near Stovepipe Wells | 7.7 | -12/40 | Medium sand | Mixed lithic fragments and quartz from Emigrant Pass to the west and Furnace Wash to the east | Major: quartz Minor: plagioclase feldspar, potassium feldspar |
| Moses Lake (47.05° N, 119.31° W) | Quincy Basin in central WA | 40 | 345/18 | Fine sand | Basaltic sand from the east bank of the Columbia River | Major: quartz, albite |
| White Sands (32.89° N, 106.33° W) | South-central NM, Tularosa Valley | 704 | 1216/10 | Fine sand | Paleo-lake Otero, present playa Lake Lucero to the southwest | Major: gypsum |

Sand dunes sites: Emissivity range



NAALSED validation with pseudo-invariant sand dune sites

| Dune site | ASTER MINUS LAB EMISSIVITY (%) | | | | | |
|-----------------|--------------------------------|---------|---------|---------|---------|-------------|
| | Band 10 | Band 11 | Band 12 | Band 13 | Band 14 | Mean |
| Algodones | 0.68 | 0.60 | 0.13 | 0.02 | 1.40 | 0.57 |
| Stovepipe Wells | 0.17 | 0.77 | 1.02 | 0.34 | 0.37 | 0.53 |
| White Sands | 0.34 | 2.76 | 0.16 | 0.92 | 1.08 | 1.05 |
| Kelso Dunes | 1.57 | 1.04 | 1.33 | 1.91 | 0.81 | 1.33 |
| Great Sands | 1.44 | 0.97 | 1.42 | 1.64 | 0.69 | 1.23 |
| Moses Lake | 0.69 | 0.52 | 0.42 | 0.61 | 1.01 | 0.65 |
| Sand Mountain | 7.74 | 6.47 | 9.01 | 1.82 | 1.10 | 5.23 |
| Coral Pink | 7.48 | 6.44 | 7.32 | 2.50 | 1.70 | 4.90 |
| Little Sahara | 3.55 | 2.39 | 2.60 | 0.96 | 0.19 | 1.94 |
| Killpecker | 2.34 | 1.99 | 2.26 | 1.33 | 0.81 | 1.75 |

< 1.6% (1 K)

GREAT SANDS, Colorado

Major: Quartz

Minor: Feldspar, magnetite



WHITE SANDS, NM
Major: Gypsum

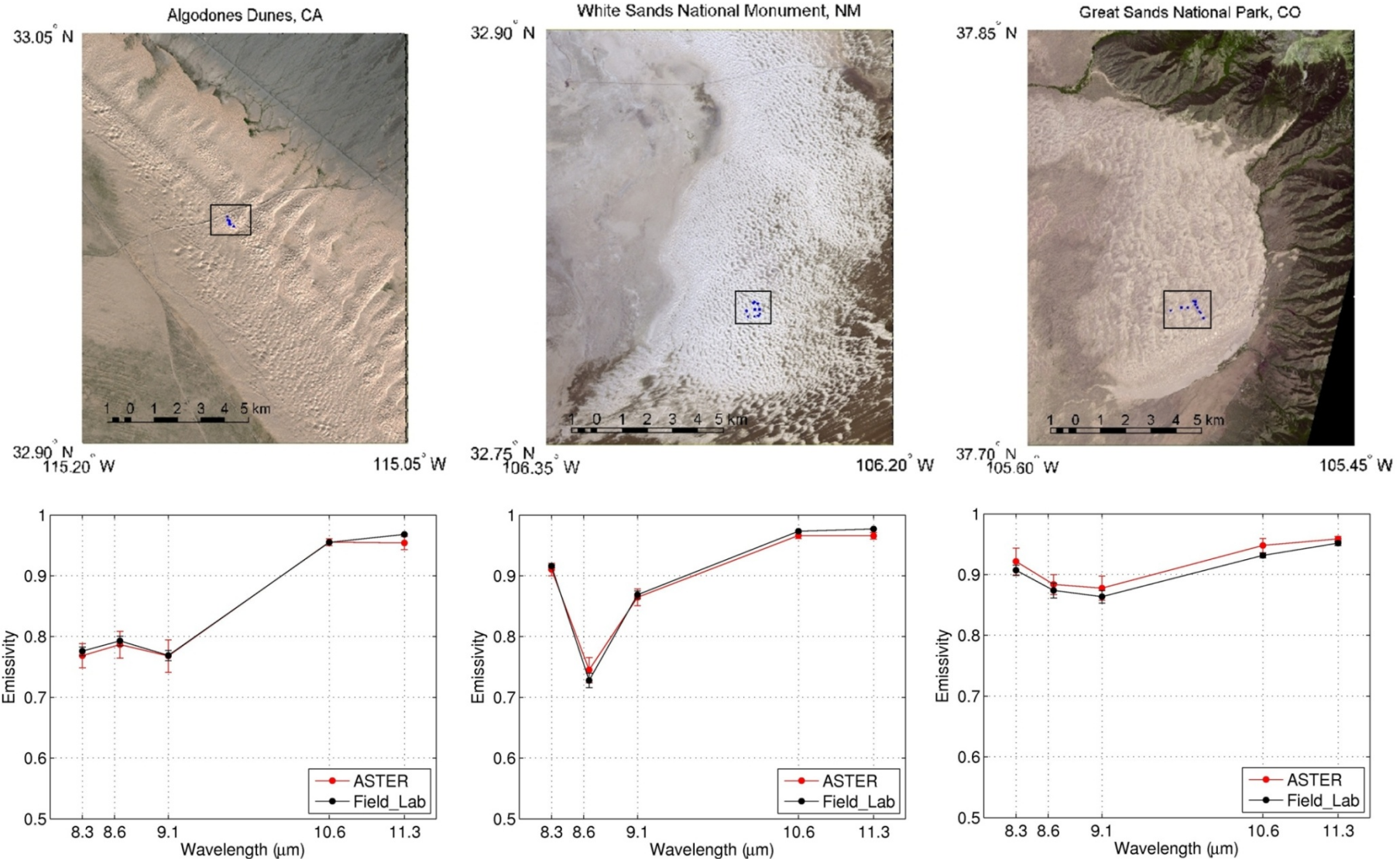


CORAL PINK SANDS, Utah

Major: Quartz



Validation of North American ASTER Emissivity Database (NAALSED)



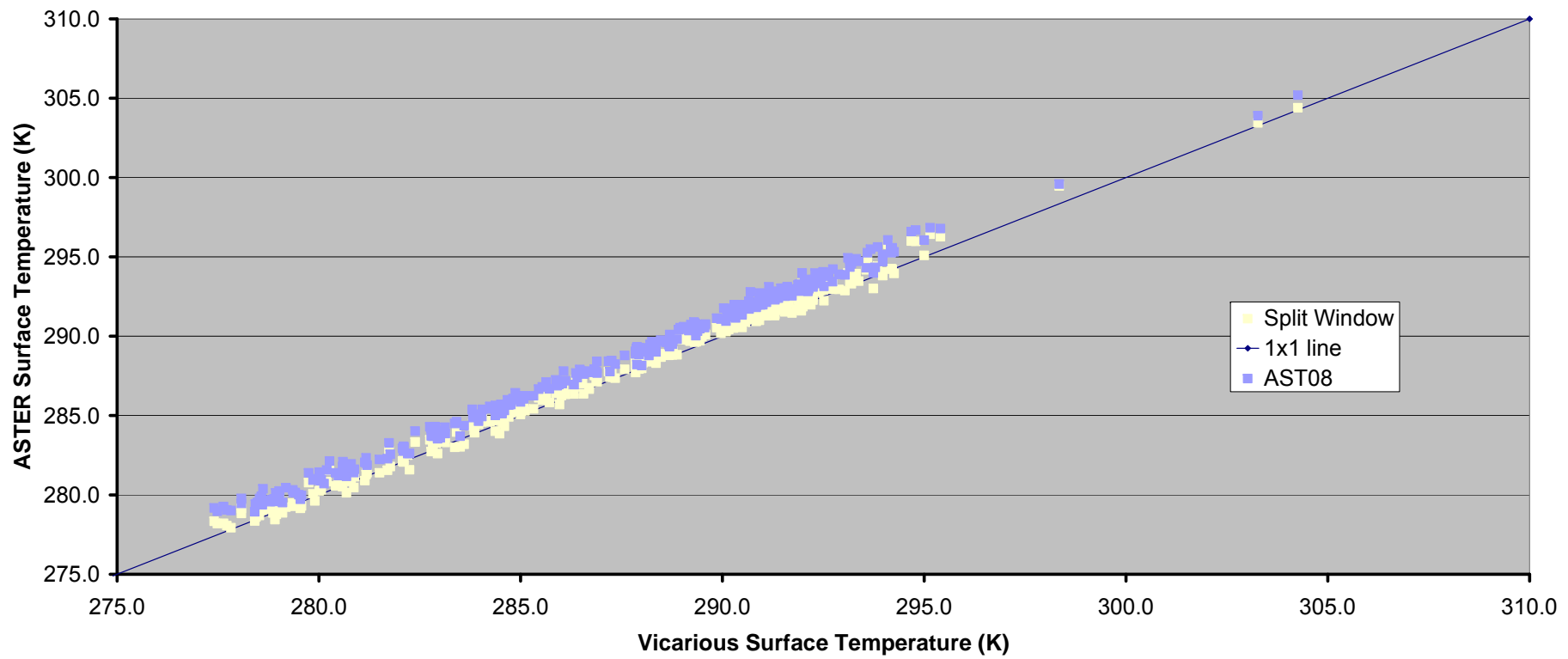
Hulley, G. C., Hook, S. J., and A.M. Baldrige, (2009), Validation of the North American ASTER Land Surface Emissivity Database (NAALSED) Version 2.0, *Remote Sensing of Environment*, 113, 2224-2233

LST Validation

- Notoriously difficult due to large spatial heterogeneity
- In-Situ ground measurements concurrent with overpass
 - Lake Tahoe and Salton Sea automatic Cal/Val facility (since 2000)
 - Rice field validation site in Valencia, Spain (full cover)
 - DOME-A site, Antarctica
 - Automated radiometer towers at sand dune sites?
- Radiance-based LST validation (MODIS)
 - Atmospheric profiles concurrent with overpass and an accurate measured emissivity are needed
 - TOA radiance estimated for two LST values close to retrieved value. 'True' LST is found by interpolating these values to observed radiance.

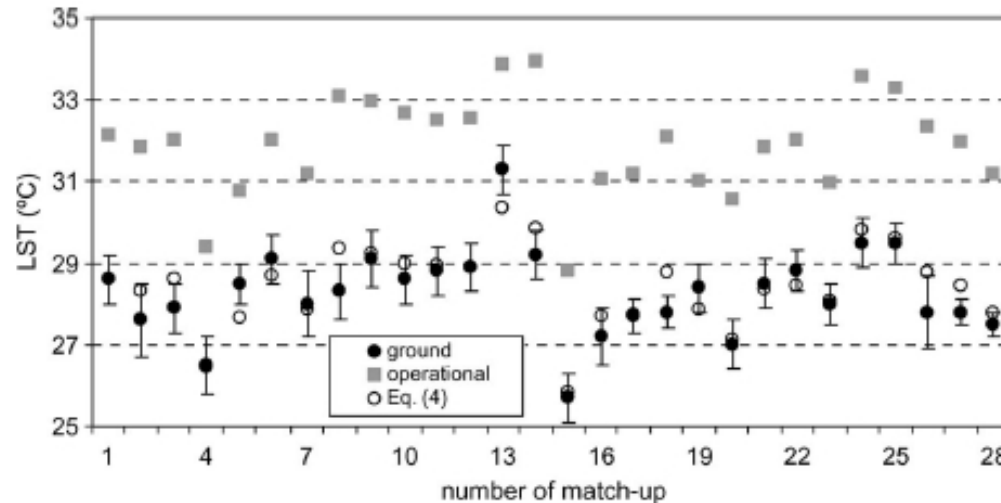
Lake Tahoe

ASTER and In Situ (Vicarious) Surface Kinetic Temperatures at Lake Tahoe and Salton Sea CY2000-2008 VZ 0-7 v4-5.x



Valencia Rice Site

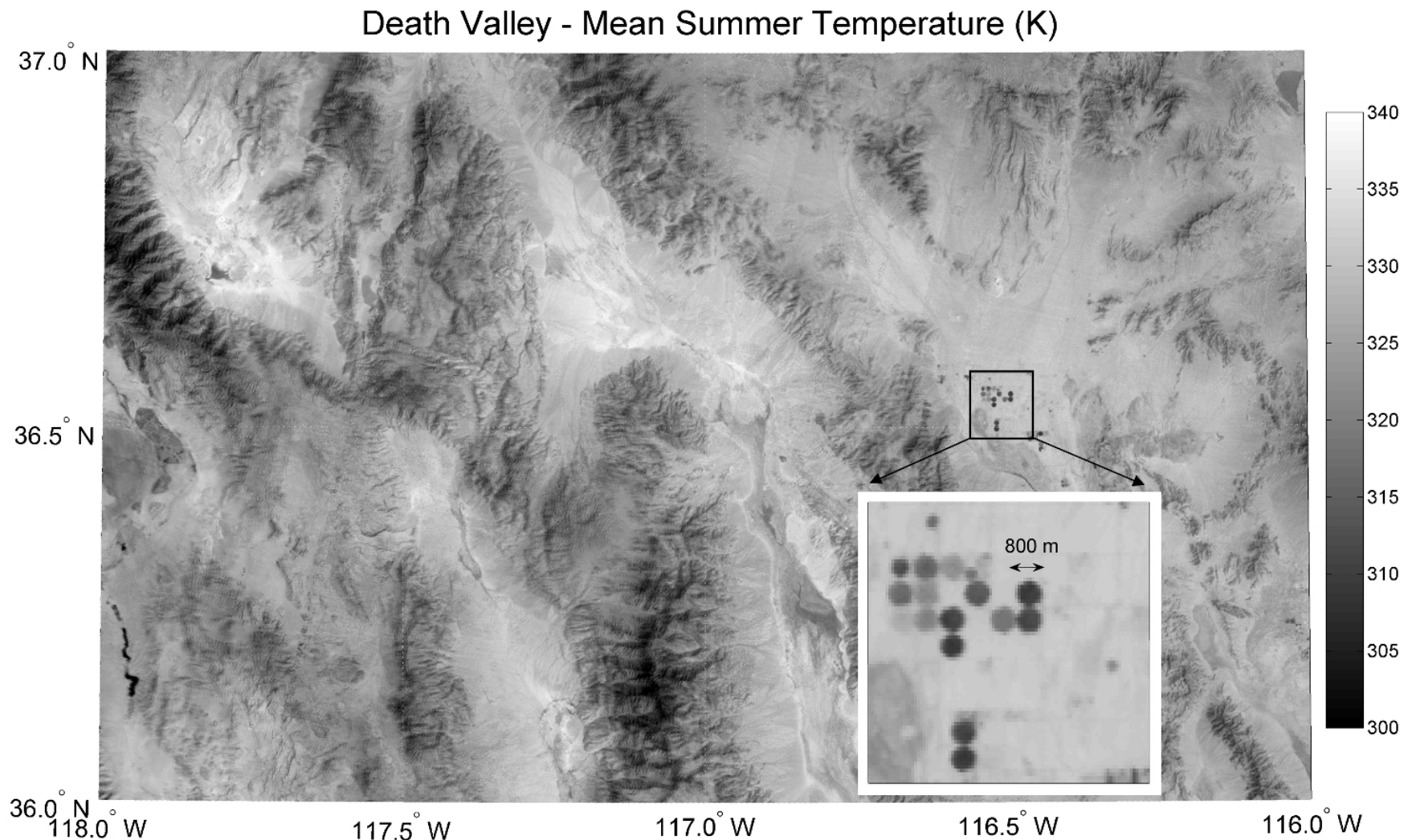
AATSR LST validation



Coll et al., (2009)

When correct biome is classified (broadleaf shrub), AATSR LST show excellent agreement with in-situ measurements ($<0.5^{\circ}\text{C}$)

NAALSED LST at 100 m – ASTER Emissivity Database



Rice crop spatially well resolved, as well as temperature differences between them

Conclusions

- Identified core L-2 Products
 - Surface Radiance
 - Land/Ocean Surface Temperature
 - Land Surface Temperature
- Identified atmospheric correction scheme
 - MODTRAN 5*
 - Water-Vapor Scaling Atmospheric Correction
- Identified LST&E algorithm
 - Temperature Emissivity Separation (TES)
 - Investigate different calibration curves and atmospheric correction techniques (WVS)
- Identified core validation sites
 - Antarctica, Valencia, Sand dunes, Tahoe/Salton Sea

Advances in Atmospheric Correction Methods

- Accuracy of atmospheric profiles are improving:
 - AIRS: 1 K/km temperature, 10% humidity
 - MODIS: ~2K temperature, 5-10% PWV, improved emissivity model using baseline-fit, Future ozone profiles, not just TOZ
- Accuracy of radiative transfer is improving, eg. MODTRAN 5 (new water molecular band model, higher spectral resolution)
- Method for improving accuracy of atmospheric correction parameters:
 - Water Vapor Scaling Method (WVS) – proposed by Tonooka (2005)
 - Coefficients available for ASTER and MODIS bands (<30 deg viewing angle)